

Dynamic Evolution of Pyramid Structures during Growth of Epitaxial Fe(001) Films

K. Thürmer, R. Koch, M. Weber, and K. H. Rieder

Freie Universität Berlin, Institut für Experimentalphysik, Arnimallee 14, D-14195 Berlin, Germany

(Received 5 April 1995)

The growth of epitaxial Fe(001) films UHV deposited onto Mg(001) substrates has been investigated at conditions where Schwoebel barriers suppress the step-down diffusion of impinging atoms. In nearly perfect agreement with the theoretical predictions of Siegert and Plischke [Phys. Rev. Lett. **73**, 1517 (1994)], scanning tunneling microscopy reveals the development of mesoscopic pyramidlike structures at the surface that grow in time according to a power law of $t^{1/4}$. The dynamic nature of the growth process favors the formation of {012} rather than {011} facets as side planes of the pyramids emphasizing, in general, the importance of kinetic versus thermodynamic stability.

PACS numbers: 61.50.Cj, 61.16.Ch, 68.55.Bd

Although the growth of thin films has been the subject of numerous investigations in the past, for the majority of film/substrate combinations it still remains an open question how to choose the growth conditions to obtain films with a specific microstructure, without doing the experiment. As long as the substrate temperature is sufficiently high so that film growth can proceed near equilibrium, useful information is provided by thermodynamics. In that case the shape of the stable nuclei formed initially depends on the respective free surface and interface energies of film and substrate, which in turn also determines the mode of film growth: 2D (layer-by-layer) or 3D (island) growth [1]. At lower substrate temperatures film growth increasingly is influenced by a variety of nonequilibrium processes, accompanied often by a change of the overall film morphology. A decisive parameter involved in nonequilibrium growth is surface diffusion, which particularly in molecular beam epitaxy (MBE) growth is the predominant mechanism for the transport of material in ordering processes. When the substrate temperature falls below a critical value, the potential barrier at step edges, often called the Schwoebel barrier [2], suppresses and ultimately inhibits the downward diffusion of atoms to the next terrace [3]. Consequently, surface diffusion is confined to the terrace where the film atoms originally impinged, until they are finally incorporated at a ledge site of an uphill terrace or form islands.

In recent years there has been growing interest in film growth where Schwoebel barriers are effective, both from a theoretical point of view [4] because of a possibly universal spatial and temporal behavior and from an experimental point of view due to its relevance for MBE growth. Schwoebel barriers have been found to be responsible for the transition from 2D growth to 3D in homoepitaxy [5], whereas here layer-by-layer growth definitely is favored by thermodynamics; 2D islands nucleate on top of pre-existing islands, resulting eventually in a time-dependent roughening of the originally flat surface [6]. By analyzing their He scattering data on the homoepitaxial growth of Cu on Cu(001), Ernst *et al.* [7] arrived at a surface pro-

file consisting of “pyramidlike” structures, whose sides correspond to Cu{113} and Cu{115} facets at 160 and 200 K, respectively. Johnson *et al.* [8] observed the formation of mounds during homoepitaxial growth of GaAs on flat substrates, whereas the original step configuration of vicinal substrates in principle is preserved. On the basis of their experimental results, as well as parallel Monte Carlo simulations, the authors were able to propose a simple analytic expression that describes the diffusion current \mathbf{j} on flat and vicinal surfaces as well. Inserting \mathbf{j} into the Langevin equation for MBE growth [4,9]

$$\partial h(\mathbf{r}, t)/\partial t = -\nabla \cdot \mathbf{j}[\nabla h(\mathbf{r}, t)] + f(\mathbf{r}, t) \quad (1)$$

then yields the 3D surface corrugation represented by the local height $h(\mathbf{r}, t)$ at position \mathbf{r} as a function of the deposition time t with $f(\mathbf{r}, t)$ being the respective beam intensity. Motivated by the work of Ref. [8], Siegert and Plischke [10] very recently derived a more sophisticated expression for the surface current that additionally accounts for the anisotropy of surface diffusion due to the symmetry requirements of the cubic lattice. Numerical solution of the resulting Langevin equation (1) reveals a surface structure consisting of a regular pattern of square pyramids with, at later growth stages, exclusively {011} facets as side planes. According to this model system the average size $\langle r(t) \rangle$ of the pyramids increases as a power law in deposition time, $\langle r(t) \rangle \sim t^{1/z}$, with $z = 4$.

In the following we present scanning tunneling microscopy (STM) results on the dynamic evolution of a *real* thin film system with effective Schwoebel barriers, namely, Fe(001) films on Mg(001), that epitaxially grow up to mean film thicknesses of more than 2000 monolayers. In nearly perfect agreement with the theoretical model of Siegert and Plischke [10] a scenery of mesoscopic and predominantly square pyramids is imaged in real space. Again in accordance with Ref. [10] the pyramids grow with a dynamic exponent of $z = 4$. At higher film thicknesses the slope of the pyramid sides converges to that of {012} facets, as confirmed by low energy electron diffraction (LEED). Obviously the {012} facets,

which are composed of (001) and {011} microfacets, attain special kinetic stability by the dynamic nature of the growth process.

The epitaxial Fe(001) films were deposited in UHV (base pressure $< 1 \times 10^{-10}$ mbar) at a deposition rate of 0.007 ± 0.001 nm/s and substrate temperatures of 400–450 K. The pressure during deposition was better than 3×10^{-9} mbar. Prior to mounting into the UHV chamber the MgO(001) substrates were baked for several hours (4–10) at 1300 K in a stream of oxygen at atmospheric pressure and briefly outgassed in UHV at 600 K immediately before film deposition. The quality of epitaxial growth was controlled by LEED as well as by measurements of the magnetic film properties [11] after the film deposition. For the STM investigations the films were transferred to a UHV chamber equipped with a UHV STM without breaking vacuum by means of a mobile UHV-transfer box.

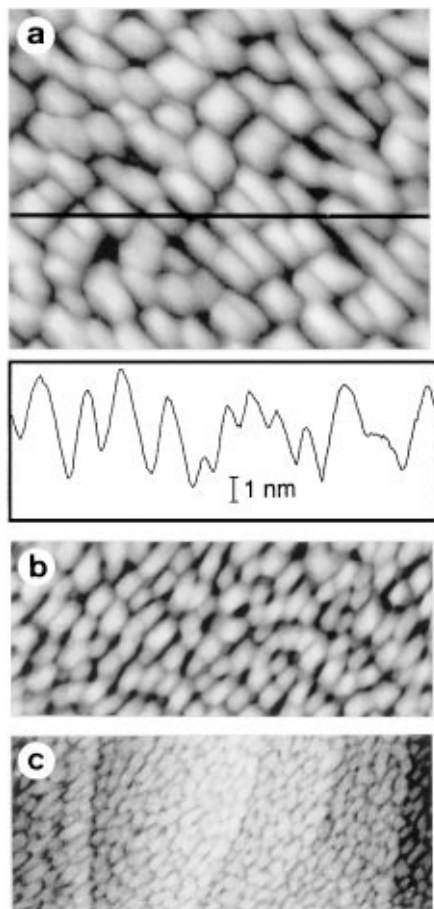


FIG. 1. Large area STM top-view images (raw data) of epitaxial Fe(001) films at different film thicknesses t_F showing pyramidlike surface structures: (a) 200×160 nm², $t_F = 300$ nm (tip voltage $U_T = -7$ V, tunneling current $I_T = 0.5$ nA), single scan is along the straight line marked in the top view; (b) 200×80 nm², $t_F = 50$ nm ($U_T = -6$ V, $I_T = 0.5$ nA); (c) 300×120 nm², $t_F = 11$ nm ($U_T = -4.5$ V, $I_T = 0.5$ nA).

In accordance with the findings of other groups [12] Fe grows epitaxially on Mg(001) substrates. The epitaxial orientation determined with LEED is Fe(001)//MgO(001) and Fe[100]//MgO[110]. The high quality of epitaxial growth is additionally corroborated by the magnetic film properties, since all Fe films exhibit a distinct magnetic in-plane anisotropy with the easy magnetization axis lying along $\langle 100 \rangle$ directions, as in the bulk [13]. Figure 1 depicts large area STM top-view images of Fe films at different thicknesses (up to 2000 monolayers) that were deposited in the temperature range of 400–450 K [14]. Obviously the surface of such Fe film is not flat. STM instead reveals that the surface is decorated over and over by a dense arrangement of predominantly square and rectangular hillocks. In three dimensions the majority of hillocks exhibits the shapes of small pyramids as

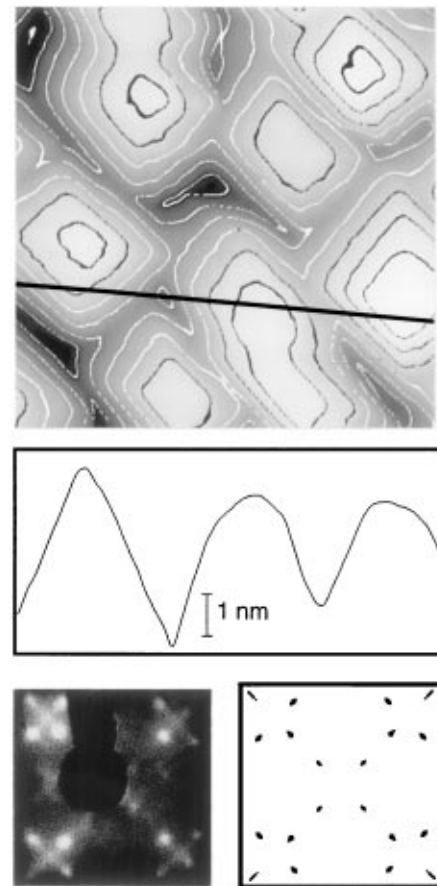


FIG. 2. Top: 65×65 nm² STM top-view image of a 300 nm thick epitaxial Fe(001) film showing the pyramidlike surface structure in detail; for better comparison with Fig. 2 of Ref. [10] contours of equal height separated by 1 nm have been added to the gray scale representation ($U_T = -7$ V, $I_T = 0.5$ nA). Middle: Single scan along the straight line marked in the top view. Bottom: Experimental (left) and calculated (right) LEED patterns of the 300 nm thick Fe(001) film (beam energy 101 eV); for the calculation by means of kinematic LEED theory a unit cell consisting of 600 atoms for each of the four {012} facets was used.

is demonstrated also by the sharp peaks in respective single scans [e.g., Figs. 1(a) and 2]. To illustrate further the 3D surface morphology, the 300 nm film is shown at higher magnification in Fig. 2. In order to facilitate the comparison with the theoretical results presented by Siegert and Plischke in their Fig. 2 (see Ref. [10]) we chose an analogous gray scale representation in combination with contours of equal height (separated by 1 nm each). The STM image of Fig. 2, which has been corrected with respect to the thermal drift during scanning, impressively elucidates the pyramidlike outlines of most islands as well as the fourfold symmetry of individual pyramids. Most pyramids are flattened at their tops; some pyramids are coalescing to finally form larger pyramids. Comparison of the STM images of Fig. 1 of Fe films at different film thicknesses t_F shows that the average pyramid size $\langle r(t) \rangle$ increases with deposition time. Quantitative evaluation of the average pyramid density N , determined from the average number of peaked structures in $100 \times 100 \text{ nm}^2$ STM images, yields a linear dependence of $\log N$ on $\log t_F$. From the slope of the straight line depicted in the double logarithmic plot of Fig. 3 a growth law $\langle r(t) \rangle \sim t^{1/4}$ ($z = 4.3 \pm 10\%$) is obtained.

The experimental results presented so far, i.e., the growth of epitaxial Fe(001) films with a surface profile represented by mesoscopic pyramidlike structures as well as the power law dependence $\langle r(t) \rangle \sim t^{1/4}$ describing the dynamic behavior of the pyramid growth, are in excellent agreement with the theoretical predictions of Siegert and Plischke [10] for film growth proceeding at conditions where Schwoebel barriers are effective. We therefore are convinced that the system Fe/MgO(001) represents a real Schwoebel system at the experimental conditions chosen. We want to emphasize that the growth of surface pyramids is not the result of a possible roughness of the MgO(001) substrates. The sharp LEED patterns obtained from the clean substrates before film deposition indicate the presence of extended well-ordered ter-

aces. An average terrace width of $\sim 50 \text{ nm}$ can be estimated from the STM top view of Fig. 1(c) of an 11 nm thick Fe film, where the original step configuration of the substrate still can be sensed beneath the significantly smaller lateral period of the pyramid structure. As the steps cannot be discerned in individual single scans the actual step height has to be very small in accordance with the maximum corrugation of about 1 nm guaranteed by the manufacturer [15]. Consequently, the formation of pyramids is inherently related to the growth of Fe itself and starts when the first 2D Fe islands have nucleated uniformly on the clean Mg(001) substrates. We recall that STM investigation of Fe films in the monolayer range is not possible on the dielectric MgO substrates as STM experiments require electrical conductance of the entire film, which therefore has to cover the substrate (with all its steps) completely. The temperature range at which Schwoebel barriers give rise to a pyramidlike surface profile is quite narrow (400–450 K; see Ref. [14]). At lower temperatures mounds with predominantly round shapes are formed that no longer reflect the fourfold symmetry of the still epitaxial Fe films; obviously the diffusivity along the step ledges then has become too low for smoothing [16]. At temperatures higher than 500 K the Schwoebel barrier is overcome and atomically flat terraces extending over several hundred nm are observed. Both findings are in agreement with the growth study on Fe/Fe(001) by Stroschio, Pierce, and Dragoset [17].

From our STM images we can also determine the crystal planes that form the sides of the pyramids, namely, by analyzing the respective slopes m of single STM scans. Whereas for thinner films still a variety of different slopes is detected, m of the thicker films ($>50\text{--}100 \text{ nm}$) measured at the lower part of the pyramids gradually converges to a value of $0.50 \pm 5\%$. Since the azimuthal orientation of the pyramids is parallel to Fe $\langle 100 \rangle$ the side planes correspond to $\{012\}$ facets, which according to crystal geometry are inclined against (001) by a ratio

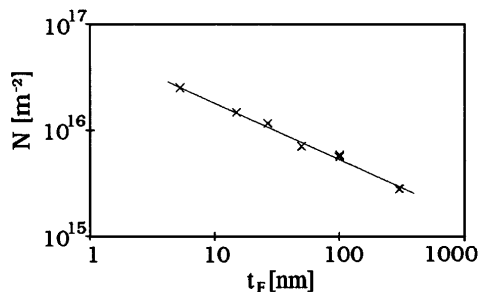


FIG. 3. Dependence of the pyramid density N (= average number of peaked structures per m^2 evaluated from $100 \times 100 \text{ nm}^2$ STM images) on the mean film thickness t_F (in nm) illustrated by a double logarithmic plot. The slope of the straight line corresponds to a growth law for the average pyramid size $\langle r(t) \rangle \sim t^{1/4}$.

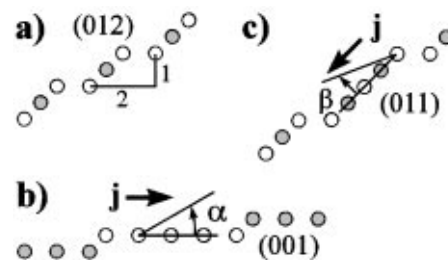


FIG. 4. (a) Sphere model of a bcc (012) surface. (b),(c) Schematic illustration of the growth of pyramidlike structures on bcc (001) and bcc (011) surfaces, respectively; α and β indicate the increase of the local slope due to anisotropic diffusion currents \mathbf{j} . Notice that due to the opposite signs of \mathbf{j} on bcc (001) and bcc (011) β corresponds to an increase relative to bcc (011) but to a decrease with respect to bcc (001).

of 1:2 [Fig. 4(a)]. The two neighboring surfaces {011} and {013} exhibit inclination values of 1:1 ($m = 1.00$) and 1:3 ($m = 0.33$), respectively, and therefore can be definitely excluded. Moreover, the STM results are confirmed by the LEED patterns, which exhibit an energy dependence characteristic of faceted surfaces (Fig. 2). Spot position as well as the intensity variation with beam energy are well reproduced by LEED patterns calculated from kinematic LEED theory assuming a unit cell consisting of 600 atoms for each of the four {012} facets (e.g., Fig. 2).

The occurrence of {012} facets as stable side planes apparently contradicts the model calculations of Siegert and Plischke. But as the authors point out in Ref. [10] the selected slope of {011} facets actually is the result of their model assumptions on the diffusion current \mathbf{j} , and may not necessarily be the only stable situation. The development of stable {012} facets in the case of Fe(001)/MgO(001) indeed may be understood in terms of the dynamic nature of the growth process. As discussed by Villain [4] the presence of extended densely packed terraces [e.g., Fe(001)] gives rise to instabilities. Both the resulting uphill current due to the diffusion to step ledges and the formation of 2D islands on terraces that are wider than the average diffusion length of the film lead to an increase of the local slope [α in Fig. 4(b)]. Ultimately it is this anisotropy of the diffusion current \mathbf{j} that is responsible for the growth of pyramidlike structures. In fact, the same mechanism inhibits the formation of extended densely packed Fe{011} facets as side planes of the pyramids. As illustrated in Fig. 4(c) Fe atoms impinging on longer {011} facets move to the next ledge site which again is accompanied by an increase of the local slope β measured relative to the respective {011} surface [Fig. 4(c)]; for nucleation of 2D islands the length of the facets probably is too small. Because of the opposite signs of the diffusion currents \mathbf{j} on (001) and (011) surfaces, however, the surface profile as a whole flattens with respect to the (001) surface [compare Figs. 4(b) and 4(c)]. Since the same mechanism destabilizes both extended (001) and {011} facets the stable situation consequently must lie *between* the two densely packed surfaces. In the case of Fe(001)/MgO(001) the steady state profile of the pyramids is formed by {012} facets that exhibit both (001) and {011} microfacets. An analogous explanation probably accounts for the formation of {113} and {115} facets in the case of Cu/Cu(001) [7]. In our opinion the experimental results presented here point to a general property of film growth at presence of Schwoebel barriers, namely, that facets are stabilized kinetically rather than by equilibrium thermodynamics.

In conclusion, by studying the growth of Fe on MgO(001) we have discovered a *real* heteroepitaxial thin film system that is characterized by the growth of pyramidlike surface structures as a consequence of Schwoebel barriers. Real space investigation with STM confirms the main theoretical predictions of Siegert and Plischke [10] concerning both structural and dynamic aspects of the growth behavior. In view of the quite regular arrangement of the pyramidlike structures we speculate whether the growth of high quality epitaxial films at conditions where Schwoebel barriers are effective might provide a new experimental approach to modify surfaces on a nanometer scale for future technological applications.

-
- [1] E. Bauer, Z. Kristallogr. **110**, 372 (1958).
 - [2] R. L. Schwoebel and E. J. Shipsey, J. Appl. Phys. **37**, 3682 (1966); R. L. Schwoebel, *ibid.* **40**, 614 (1969).
 - [3] G. Ehrlich and F. G. Hudda, J. Chem. Phys. **44**, 1039 (1966); G. Ehrlich, Phys. Rev. Lett. **70**, 41 (1993).
 - [4] J. Villain, J. Phys. I (France) **1**, 19 (1991).
 - [5] R. Kunkel, B. Poelsema, L. K. Verheij, and G. Comsa, Phys. Rev. Lett. **65**, 733 (1990).
 - [6] Y.-L. He, H.-N. Yang, T.-M. Lu, and G.-C. Wang, Phys. Rev. Lett. **69**, 3770 (1992).
 - [7] H.-J. Ernst, F. Fabre, R. Folkerts, and J. Lapujoulade, Phys. Rev. Lett. **72**, 112 (1994).
 - [8] M. D. Johnson, C. Orme, A. W. Hunt, D. Graff, J. Sudijono, L. M. Sander, and B. G. Orr, Phys. Rev. Lett. **72**, 116 (1994).
 - [9] M. Siegert and M. Plischke, Phys. Rev. E **50**, 917 (1994).
 - [10] M. Siegert and M. Plischke, Phys. Rev. Lett. **73**, 1517 (1994).
 - [11] M. Weber, R. Koch, and K. H. Rieder, Phys. Rev. Lett. **73**, 1166 (1994).
 - [12] T. Kanaji, K. Asano, and S. Nagata, Vacuum **23**, 55 (1973); T. Urano and T. Kanaji, J. Phys. Soc. Jpn. **57**, 3403 (1988).
 - [13] R. Koch, M. Weber, K. Thürmer, and K. H. Rieder (to be published).
 - [14] In that temperature range no dependence of the film morphology on the deposition temperature was observed (compare also the results of Fig. 3). The deposition temperature was detected via pyrometry with a relative accuracy of ± 10 K; we note, however, that the absolute error of the substrate temperature may be as high as ± 30 K due to the experimental difficulty of temperature measurements on dielectric substrates.
 - [15] Crystal GmbH, Ostendstrasse 1-14, D-12459 Berlin.
 - [16] H. Brune, C. Romainczyk, H. Röder, and K. Kern, Nature (London) **369**, 469 (1994).
 - [17] J. A. Stroschio, D. T. Pierce, and R. A. Dragoset, Phys. Rev. Lett. **70**, 3615 (1993).